EFFECTS OBSERVED UNDER MONOTONIC-CYCLIC LOADING COMBINATIONS: EXPERIMENT AND MODELLING

Zbigniew L. Kowalewski, zkowalew@ippt.pan.pl
Institute of Fundamental Technological Research, ul. Pawinskiego 5B, 02-106 Warsaw, Poland

Tadeusz Szymczak, tadeusz.szymczak@its.waw.pl
Motor Transport Institute, ul. Jagiellonska 80, 03-301 Warsaw, Poland

Jan Maciejewski, jan.maciejewski@simr.edu.waw.pl
Warsaw University of Technology, ul. Narbutta 84, 02-524 Warsaw, Poland

Abstract. *The effects often taking place during proportional and non-proportional types of loading were identified experimentally and modelled numerically. In the case of non-proportional cyclic loading along circular strain path the second order effects such as: phase shift between stress and strain signals were discovered. An analysis of experimental data from tests under non-proportional cyclic loading along square strain path exhibited a significant reduction of stress independently on direction of deformation. The paper also presents experimental results concerning evaluation of an influence of cyclic loading on mechanical parameters during monotonic deformation carried out on the 2024 aluminium alloy and X10CrMoVNb9-1 steel. All strain-controlled tests were conducted at room temperature using thin-walled tubular specimens. The experimental programme contained selected combinations of monotonic and cyclic loadings, i.e. the torsion-reverse-torsion cycles were superimposed on the monotonic tension. It is shown that such cycles caused essential variations of the tension characteristics. A significant decrease of the tension stress was observed. The effects occured during monotonic and cyclic loading combinations were described using Mróz and Maciejewski model. Reasonable good predictions of: hysteresis loops and stress responses for the square and circular loading paths and tensile curves assisted by torsion cycles were obtained.*

Keywords*: cyclic loading, hardening, softening, complex stress state*

1. INTRODUCTION

Mechanical behaviour of structural materials under different kinds of cyclic loading is a topic which was studied in the past by many research teams, e.g. (Lamba and Sidebottom, 1978; Tanaka et al., 1985; Benallal and Marquis, 1987). Even now it is still under consideration, e.g. Kowalewski and Szymczak (2012, 2014); Shamsei et al. (2010). Previous results demonstrated an additional hardening of the material expressed by much higher stress level at saturation state during deformation along circular loading path than that for simple tension-compression cycles observed (Lamba and Sidebottom, 1978). Similar phenomenon was also well reflected for the 316 stainless steel (Tanaka et al. 1985). An influence of various type of loading paths, i.e. proportional and non-proportional on the same material was examined by Calloch and Marquis (1997). They analysed maximum equivalent stress at steady state for: tension-compression, hourglass, cruciform, square and circular paths. The largest value of the stress equal to 570MPa was obtained during deformation along circular path, but the smallest one of 350MPa was achieved for tension-compression.

From previous experimental investigations it is also known that for certain class of materials the softening effect can be observed under non-proportional cyclic loadings (Lamba and Sidebottom, 1978; Shamsei et al., 2010). Such difference between material behaviour under cyclic loading leads to the essential difficulties in the constitutive modelling. Therefore, for the rational formulation of multiaxial cyclic constitutive equation, it is necessary to study a series of representative non-proportional cyclic tests, and to identify the property of the multiaxial cyclic hardening/or softening mechanisms. In this paper the representative results will be given.

Among many topics taking place in analysis of cyclic loading effects in engineering materials one can distinguish experimental evaluation of an influence of different forms of shear deformation of engineering materials on their mechanical parameters variation during parallel or subsequent loading processes (Kong and Hodgson, 2000; Bochniak and Korbel, 2003; Kowalewski and Szymczak, 2012, 2014). The results achieved from such investigations are important from technological point of view because they are providing a knowledge necessary for modification of some metal forming processes, such as forging, drawing or extrusion. This is also an issue addressed in the paper.

2. EXPERIMENTAL DETAILS

The experimental programme of tests on thin-walled tubular specimens, Fig. 1, comprised two essential parts:

(a) tension-torsion cycles to form the circular and square strain paths, Fig. 2,
(b) combination of monotonic tension and torsion-reverse-torsion cycles, Fig. 3.

The 2024 aluminium alloy commonly used in aircraft industry was employed to determine the material behaviour due to deformation path along the circle. The circular path amplitude achieved the following values i.e.: ±0.2%, ±0.4%, ±0.6%, ±0.8%.

The X10CrMoVNb9-1 steel widely used for pipes in the construction of power plant components that operate under high temperature and complex stress conditions was selected for investigations under monotonic tension and torsion cycles.

All experiments were performed in the biaxial stress state produced within thin wall of the tubular specimen (Fig. 1) by the application of an axial and shear strain signals (Figs. 2, 3) using the servo-hydraulic testing machine. The strain gauges were cemented to the outer surface of the specimen and located near the terminal with strain gauges wired to form three temperature compensated bridge circuits corresponding to the appropriate strain components.

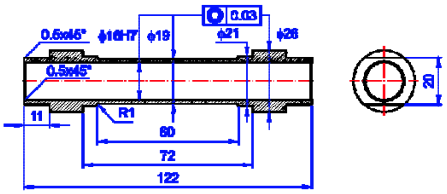

Figure 1. Thin-walled tubular specimen

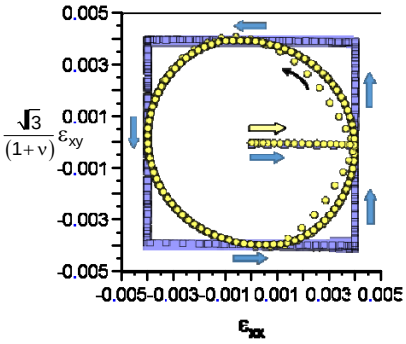

Figure 2. Circular and square strain paths for the cyclic strain amplitude of ±0.4%

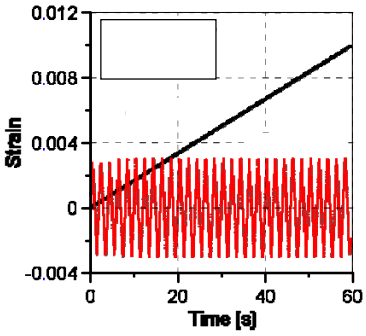

Figure 3. Monotonic tension combined with cyclic torsion

3. THE RESULTS OF TESTS UNDER COMPLEX STRAIN PATHS

3.1. Material behaviour due to non-proportional strain paths

Figure 4 illustrates in the stress plane the 2024 aluminium alloy responses into the strain controlled non-proportional cyclic loading along circular paths at four values of total strain amplitude equal of ±0.2% (1); ±0.4% (2); ±0.6% (3), ±0.8% (4). The Poisson ratio for the alloy was assumed to be 0.33 for elastic and plastic strain ranges considered. For the strain amplitude of ±0.2% (1); ±0.4% (2) neither the softening nor hardening is manifested. Such a situation is related from the fact that the just indicated strain amplitudes considered in the programme correspond to the elastic stress range. For the higher value of strain amplitude the material hardening is clearly visible, Fig. 5. This phenomenon is expressed by a gradual increase of the stress amplitude in the first cycles tending to constant value for the last one.

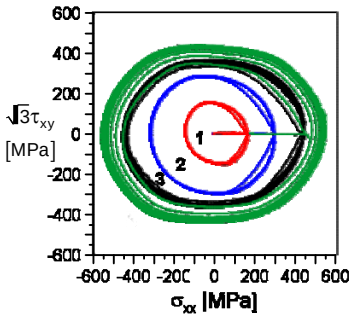

Figure 4. Stress response to the total strain controlled non-proportional cycles along circular path with strain amplitude equal to: ±0.2% (1); ±0.4% (2); ±0.6% (3), ±0.8% (4)

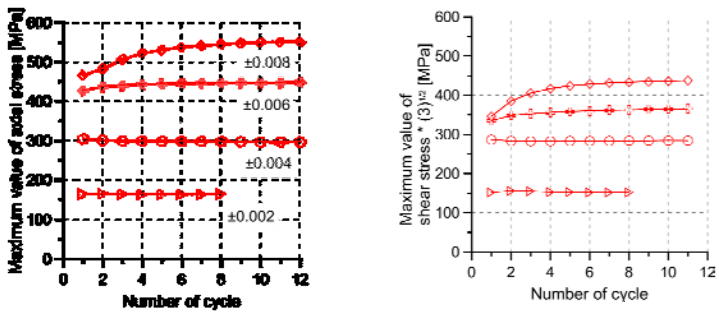

Figure 5. Maximum peaks of axial and shear stresses during circular cycles of the 2024 aluminium alloy; tests carried out under frequency of 0.025Hz

A graphical presentation of the registered signals of strain and stress components as a function of time reveals remarkable phase shift between corresponding components of strain and stress, Fig. 6. A difference between a time corresponding to the strain peak and that to the stress peak in a cycle defines so called retardation time. This phenomenon has not been sufficiently exposed in previous publications. It seems that it may be responsible for an

additional hardening/softening effect in materials undergoing to non-proportional loading in comparison to the material behaviour usually observed for proportional one.

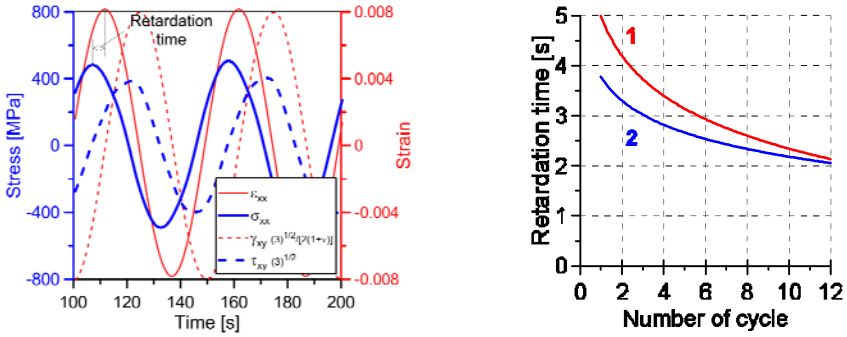

Figure 6. The results of non-proportional loading along the circular strain path for the strain amplitude of ±0.8%: (a) stress and strain signal components versus time; (b) retardation time as a function of cycle number, numbers 1 and 2 denote the results for axial and shear components, respectively

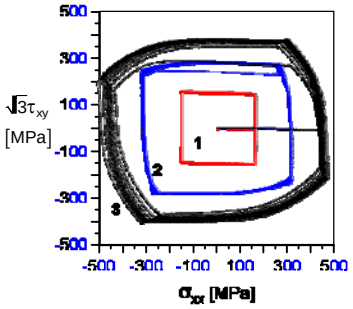

Figure 7. Stress response into the square strain path for the amplitude equal to: ±0.2% (1); ±0.4% (2); ±0.6% (3)

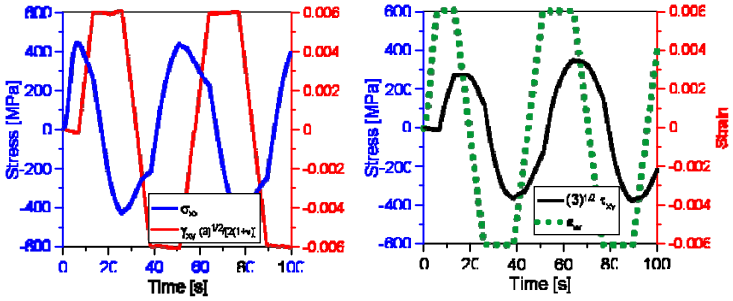

Figure 8. Variations of the strain and stress signals due to non-proportional cyclic loading along the square strain path

In the next step of experimental programme non-proportional cycles along square strain path were carried out. The main purpose of the programme was focused on identification of second-order effects (Figs. 7, 8) associated to the non-proportional cyclic loading along this shape of strain path. The control signals were designed to form a square in the strain plane. It was executed by the combination of two trapezoidal loading signals mutually delayed.

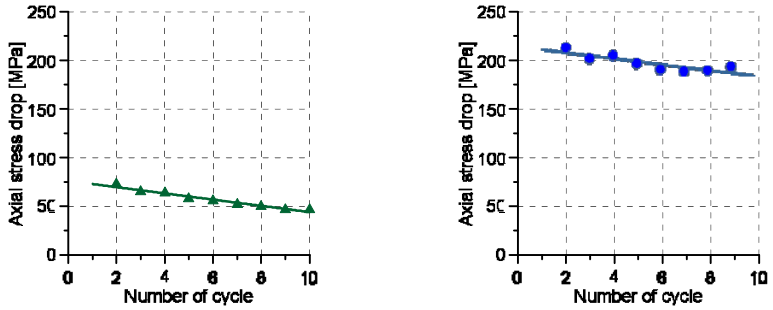

Figure 9. Axial stress drop versus cycle number during deformation along square strain path for the amplitude equal to ±0.4% (a) and ±0.6% (b)

An interesting feature can be easily noticed looking at the courses of stress and strain signals, Fig. 8. A significant reduction of stress components magnitude can be observed. It is visible when the one of the control loading signals (axial strain for example) changes a direction. The second-order effects mentioned above are especially considerable when the amount of strain amplitude increases. For example, in the case of the cyclic strain amplitude equal to ±0.4% a reduction of the axial stress was equal around 70 MPa, whereas for ±0.6% it almost achieved a level of 220 MPa, Fig. 9.

It is easy to conclude that the level of axial stress drop decreases with number of cycles. It has the linear character of variation with an increase of cycle number independently on the cyclic strain amplitude, Fig. 9a ,b.

3.2. An effect observed in tension direction due to torsion cycles assistance

An influence of the cyclic shear strain amplitude within a range from ±0.3% to ±0.7% on monotonic tension was investigated for the X10CrMoVNb9-1 steel, Fig. 10. As it is illustrated in Fig. 10, the torsion-reverse-torsion cycles caused variations of the tensile characteristics. A significant decrease of the axial stress can be observed. An increase of the cyclic strain amplitude led to the higher decrease of the tensile stress. It is expressed for example by an axial stress drop from 475 MPa to 125 MPa for the axial plastic strain equal to 0.2%.

Energy balance calculations were performed to compare total strain energy dissipated during typical monotonic test and that of a monotonic-cyclic loading combination, Fig. 11. Variations of the total strain energy calculated on the basis of tensile curves determined without or with torsion cycles exhibit a non-linear character, Fig. 11a. It decreases with an increase of the magnitude of cyclic strain amplitude, Fig. 11a (line 1). Total strain energy was also evaluated for the first cycle of torsion-reverse-torsion for each strain amplitude considered in the programme, Fig. 11 (line 2). It increases with increasing of the magnitude of cyclic strain amplitude.

Certain important remarks can be formulated after analysis of the total strain energy calculated as a sum for tensile curve and hysteresis loops for 30 cycles, Fig. 11b. For greater amplitudes of cyclic strain the total strain energy increases achieving almost a level of 200MJ/m^3. Despite of the total strain energy increasing with an increase of the cyclic strain amplitude it is worth to emphasise that superimposing cyclic torsion on monotonic tension reduces the axial stress significantly. In many industrial applications such reduction would extend the lifetimes of some engineering components. It is especially important during production of elements for which manufacturing costs are extremely high.

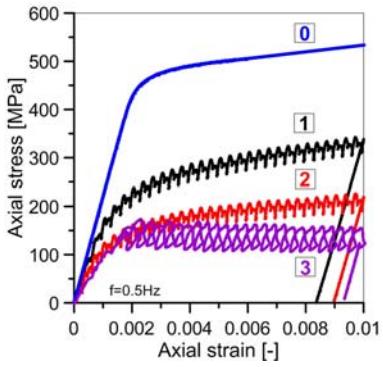

Figure 10. Comparison of typical tensile characteristic (0) with stress-strain curves from tests conducted under monotonic tension assisted by torsion cycles for strain amplitude equal to: ±0.3% (1), ±0.5% (2), ±0.7% (3)

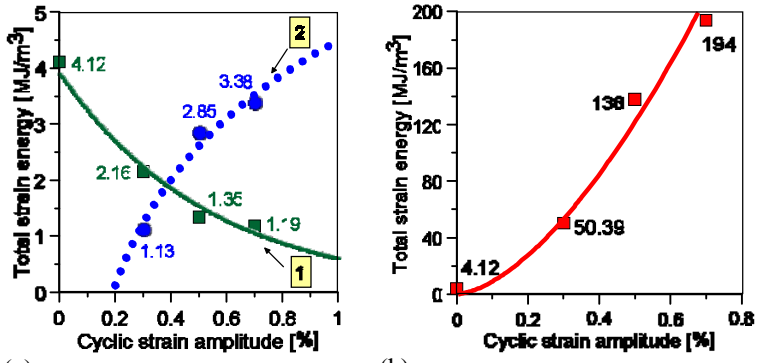

(a) (b)

Figure 11. Variations of total strain energy as a function of cyclic strain amplitude calculated on the basis of: (a) tensile curve line 1, and hysteresis loop at first cycle - line 2; (b) tensile curve and hysteresis loops for 30 cycles

4. PREDICTION OF MATERIAL BEHAVIOUR USING THE THREE SURFACE MODEL

The cyclic hardening model elaborated by Maciejewski and Mróz (2008) was applied. It is based on the classical Huber-Misses yield function and the kinematic hardening rule proposed by Armstrong and Frederick (1966). The small strain framework is assumed. This is justified by the domain of application to cyclic loading conditions. The partition of total strain tensor into an elastic strain and plastic strain, where elasticity is described by linear Hooke's Law, is considered. The yield condition and the plastic flow rule are as following:

$$f_p = \sqrt{\tfrac{3}{2}(\boldsymbol{S}-\boldsymbol{X})\cdot(\boldsymbol{S}-\boldsymbol{X})} - \sigma_p(\xi) = 0; \quad \dot{\boldsymbol{\varepsilon}}^p = \dot{\lambda}\frac{\partial f_p}{\partial \sigma} = \dot{\lambda}\frac{\tfrac{3}{2}(\boldsymbol{S}-\boldsymbol{X})}{\sigma_p}; \quad \dot{\lambda} \geq 0, \quad f_p \leq 0, \quad \dot{\lambda} f_p = 0, \tag{1}$$

where $\dot{\lambda} = \sqrt{\tfrac{2}{3}\dot{\boldsymbol{\varepsilon}}^p \cdot \dot{\boldsymbol{\varepsilon}}^p}$, $\boldsymbol{S}$ is the stress deviator, $\boldsymbol{S} = \sigma - \tfrac{1}{3}\operatorname{tr}\sigma\,\boldsymbol{1}$, $\boldsymbol{X}$ is the back stress tensor and σ_p is the yield stress. Here dot between two vectors or tensors denotes their scalar product and dot over a symbol denotes the rate with respect to a process evolution parameter. The back stress evolution rule can be written in the form

$$\dot{\boldsymbol{X}} = \dot{\lambda}\gamma(\boldsymbol{S}_I - \boldsymbol{S}) = \dot{\lambda}\gamma(\boldsymbol{X}_I - \boldsymbol{X}) = \dot{\lambda}\gamma\rho\Delta, \tag{2}$$

where γ is material parameter and $\boldsymbol{S}_l$ and $\boldsymbol{X}_l$ are the saturation states associated with the instantaneous plastic strain rate orientation. Considering a deformation process with constant orientation of the plastic strain rate vector, the stress $\boldsymbol{S}$ tends to its limiting value $\boldsymbol{S}_l$ (on the hardening surfaces F_h=0) coaxial with the plastic strain trajectory for specified $\dot{\varepsilon}^p$ of constant orientation, Fig 12. Consider now a more general model for which the hardening surface is allowed to translate and expand. We assume the hardening surface equation in the form

$$F_h = \sqrt{\tfrac{3}{2}(\boldsymbol{S}_l - \boldsymbol{Y})\cdot(\boldsymbol{S}_l - \boldsymbol{Y})} - \sigma_l(\xi) = 0\,, \tag{3}$$

and its translation rule in similar form to (2) giving the equation (4a), where $\boldsymbol{Y}$ is the second level back stress, γ_1 is the material parameter, and $\boldsymbol{Y}_l$ is the limit convergence point. Assuming that $\boldsymbol{Y}_l$ lies on the limit surface its equation can be written in the form (4b)

$$\begin{aligned} \dot{\boldsymbol{Y}} &= \dot{\lambda}\gamma_1(\boldsymbol{Y}_l - \boldsymbol{Y}) \quad for \quad r = \sqrt{\tfrac{3}{2}\boldsymbol{X}\cdot\boldsymbol{X}} > R_l\,, \\ \dot{\boldsymbol{Y}} &= \dot{\lambda}\gamma_1(\boldsymbol{X} - \boldsymbol{Y}) \quad for \quad r \le R_l\,, \end{aligned} \qquad F_y = \sqrt{\tfrac{3}{2}\boldsymbol{Y}_l\cdot\boldsymbol{Y}_l} - R_l(\xi) = R - R_l = 0, \tag{4a, b}$$

where R_l is the limit surface radius. The translation rule of the first level back stress $\boldsymbol{X}$ can be modified and instead of (2), we can assume that

$$\overset{\circ}{\boldsymbol{X}} = \dot{\lambda}\gamma(\boldsymbol{X}_l - \boldsymbol{X}) + \overset{\circ}{\boldsymbol{Y}}, \tag{5}$$

where $\overset{\circ}{\boldsymbol{Y}}$ is now the convective rate. We assume that both limit, hardening and yield surfaces expand, but the ratio of their diameters is constant, thus

$$k_l = \frac{\sigma_l}{R_l} = const, \qquad k_p = \frac{\sigma_l}{\sigma_p} = const. \tag{6}$$

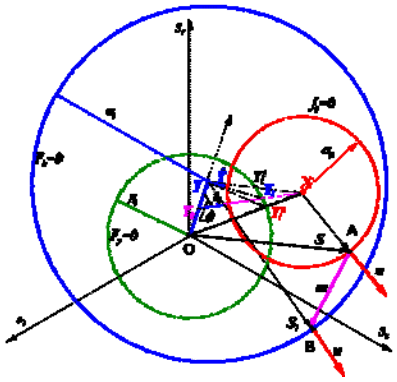

Figure 12. Concept of the three-surface model of Mróz-Maciejewski

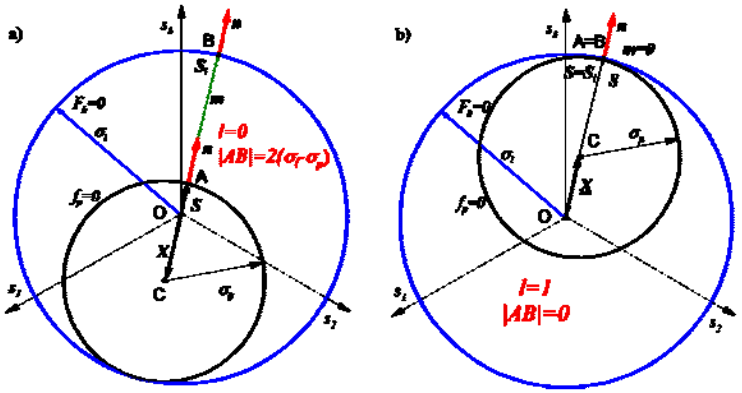

Figure 13. Translation of the yield surface along the AB path; a) initial position: l=0, $|AB|=2(\sigma_l-\sigma_p)$; b) ultimate position: l=1, $|AB|$=0

The isotropic expansion of surfaces F_h=0, f_p=0, F_y=0 is dependent on the amplitude of cyclic stress. Assuming that there is no isotropic hardening effect for $l \le l_0$, Fig.13, we can write

$$\dot{\xi} = \begin{cases} \dot{\lambda}\left(\dfrac{l-l_0}{1-l_0}\right)^{\kappa} = L^{\kappa} & , \; l > l_0; \\ 0 & , \; l \le l_0 \end{cases} \qquad l = 1 - \frac{|\Delta|}{2(\sigma_l - \sigma_p)}, \quad \Delta = |AB| = |\boldsymbol{S}_l - \boldsymbol{S}|\,. \tag{7}$$

The weighting parameter l depends on the distance of the stress point to the hardening surface. When the yield surface approaches the hardening surface, then $l \to 1$, but for the other cases there is $0 \le l \le 1$. Thus, the deformation paths more distant from the hardening surface induce lower hardening than the paths approaching the surface F_h=0. Similarly, the cycles of lower stress or strain amplitudes correspond to lower hardening rates than the cycles of higher amplitudes.

The Mróz-Maciejewski model was applied to simulate hysteresis loop variations during deformation of the 2024 aluminium alloy along square strain path with strain amplitude equal to 0.6%, Fig. 14. This concept enabled to reproduce reasonable important effects related with a square loading path, i.e. a rapid stress drop and distortion of stress response. The model was also used to predict behaviour of the X10CrMoVNb9-1 steel during monotonic-cyclic loading, Fig. 15. The material parameters have been calibrated using data from cyclic pure tension and torsion tests. The model parameters for three yield surface concept are: E = 200 GPa, ν = 0.30, hardening surface radius - σ_{l0} = 520 MPa, σ_{lf} = 540 MPa, l_0 = 0.5, κ = 1, w=1, k_p = 1.81, k_l = 4.0, and translation rule parameters γ = 550, γ_1 = 55, f = 1.

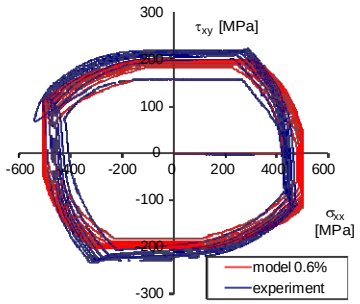

Figure 14. Comparison of numerical predictions and experimental data for cycles along square paths

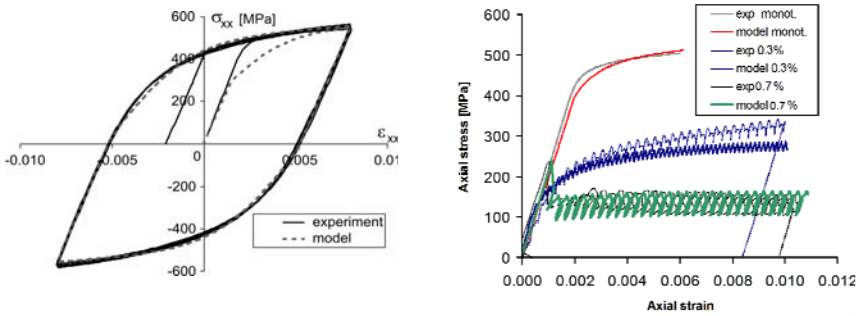

Figure 15. Comparison of the three-surface model predictions with experimental data of the X10CrMoVNb9-1 steel, a) tension-compression cycles, b) tensile curves obtained using the loading programme shown in Fig. 3

The experimental results in Fig. 15 are compared with predictions obtained using the three-surface model for strain amplitude equal γ_m=0.6% and γ_m= 1.4%. As it is clearly seen the model enables to reproduce hysteresis loops, Fig. 15a. Also, it can predict experimental response curves for all cyclic strain amplitudes considered, Fig. 15b. Therefore, the three-surface model provides realistic predictions and can be applied to simulate cyclic response of the X10CrMoVNb9-1 steel.

4. SUMMARY

The phase shift between strain and stress signals is typical feature of a material subjected to cyclic loading along circular strain path. A drop of axial and shear stresses occurs during deformation along square loading paths. The total strain energy during tension may be reduced by increasing cyclic shear strain amplitude. The Mróz-Maciejewski model can be used to simulate tension assisted by cyclic torsion. Also, it can capture the phase shift effect under non-proportional cyclic loading along circular strain paths.

5. REFERENCES

Armstrong, P.J., Frederick, C.O., 1966. "A mathematical representation of the multiaxial Bauschinger effect". CEGB Report RD/B/N731, Berkeley Nuclear Laboratories.

Benallal, A., Marquis, M., 1987. "Constitutive equations for non-proportional cyclic elasto-viscoplasticity". Trans. ASME J. Eng. Mat. Tech., Vol. 109, pp. 326-335.

Bochniak, W., Korbel, A., 2003. "KOBO – type forming: forging of metals under complex conditions of the process". J. Mat. Process. Tech., Vol. 134, pp. 120-134.

Calloch, S., Marquis, D., 1997. "3D experimental and numerical investigations to test constitutive equations for non-proportional cyclic plasticity", Transaction of the 14th International Conference on Structural Mechanics in Reactor Technology (SMiRT 14), Lyon, France, August 17-22.

Kong, L.X., Hodgson, P.D., 2000. "Constitutive modelling of extrusion of lead with cyclic torsion", Mater. Sci. Eng. A, Vol. 276, No. 1-2, pp. 32-38.

Kowalewski, Z.L., Szymczak, T., Maciejewski, J., 2014. "Material effects during monotonic-cyclic loading". Int. J. Solid Struct., Vol. 51, No. 3-4, pp. 740-753.

Lamba, H.S., Sidebottom, O.M., 1978. "Cyclic plasticity for non-proportional paths". Trans. ASME J. Eng. Mat. Tech., Vol. 100, pp. 96-111.

Maciejewski, J., Mróz, Z., 2008. "An upper-bound analysis of axisymmetric extrusion assisted by cyclic torsion". J. Mater. Process. Tech. 206, pp. 333-344.

Shamsei, N., Fatemi, A., Socie D.F., 2010. "Multiaxial cyclic deformation an non-proportional hardening employing discriminating load paths", Int. J. Plasticity, Vol. 26, pp. 1680-1701.

Szymczak, T., Kowalewski, Z.L., 2012. "Variations of mechanical parameters and strain energy dissipated during tension-torsion loading", Archives of Metallurgy and Materials, Vol. 57, No. 1, pp. 193-197.

Tanaka E., Murakami S., Oöka M., 1985. "Effects of plastic strain amplitudes on non-proportional cyclic plasticity", J. Mech. Phys. Solids, Vol. 33, No. 6, pp. 559-575.

6. RESPONSIBILITY NOTICE

The authors are the only responsible for the printed material included in this paper.